



## Short communication

Nanohybrid PVA/ZrO<sub>2</sub> and PVA/Al<sub>2</sub>O<sub>3</sub> electrospun mats

F.R. Lamastra<sup>a,b,\*</sup>, A. Bianco<sup>a,b</sup>, A. Meriggi<sup>a,b</sup>, G. Montesperelli<sup>a,b</sup>,  
F. Nanni<sup>a,b</sup>, G. Gusmano<sup>a,b</sup>

<sup>a</sup> Dipartimento di Scienze e Tecnologie Chimiche, Università di Roma "Tor Vergata",

Via della Ricerca Scientifica, 00133 Roma, Italy

<sup>b</sup> UdR INSTM "Roma Tor Vergata", Italy

## ARTICLE INFO

## Article history:

Received 22 April 2008

Received in revised form 17 July 2008

Accepted 21 July 2008

## Keywords:

Electrospinning

PVA/ZrO<sub>2</sub>

PVA/Al<sub>2</sub>O<sub>3</sub>

Nanohybrid

Mechanical properties

Microstructure

## ABSTRACT

Fibrous poly(vinyl alcohol)/zirconia and poly(vinyl alcohol)/alumina nanohybrids were obtained by electrospinning technique, the applied voltage ranging between 12 and 16 kV. The actual nanofiller content ranged between 2 and 9 wt%. Electrospun nanohybrids consisted of uniform fibers free of defects. The average fiber diameter was around 600 nm for all electrospun mats. Nano and/or submicrometric ceramic agglomerates were observed onto and inside the overall polymeric fibers. Nanohybrid mats containing the highest amounts of nanoparticles showed a significant reduction of crystallinity. All electrospun nanohybrids evidenced improved mechanical properties with respect to the neat PVA mat. The tensile modulus of PVA/Al<sub>2</sub>O<sub>3</sub> and PVA/ZrO<sub>2</sub> mats reached 350 ± 40 MPa and 190 ± 55 MPa, respectively, the value for the neat PVA being 90 ± 20 MPa.

© 2008 Elsevier B.V. All rights reserved.

## 1. Introduction

Organic–inorganic nanohybrids have recently received great attention. The idea is to combine advantages of organic materials (i.e. light weight and flexibility) and inorganic materials (i.e. mechanical strength, thermal stability and chemical resistance) [1]. Electrospinning technique allows to produce micro- to nano-fibrous mats using an electrostatically driven jet of polymer solution or polymer melt [2]. Recently, several research groups proposed studies on polymeric, composite and ceramic nanofibers processed by electrospinning [3].

Poly(vinyl alcohol) (PVA) has been largely studied due to its good film forming ability, high hydrophilicity, biocompatibility, good chemical resistance and interesting mechanical properties [4]. These properties have led to a wide range of industrial products such as membrane, textile sizing and finishing, adhesive, coatings and paints [4]. Lately, the attention has been focused on its promising biomedical applications such as drug delivery systems [5], filters [6], scaffolds for tissue engineering [7], and artificial organs [8].

The introduction of ceramic nanofiller, particularly ZrO<sub>2</sub> and Al<sub>2</sub>O<sub>3</sub>, leads to nanocomposites with improved mechanical properties, higher thermal stability and reduced water solubility [4].

In this work, nanohybrid fibrous poly(vinyl alcohol)/zirconia and poly(vinyl alcohol)/alumina mats were successfully realized by electrospinning starting from aqueous PVA solutions containing different amounts of zirconia or alumina nanoparticles. The actual content of nanoparticles in hybrid samples was determined by thermogravimetry (TG). The morphology of electrospun mats was examined by scanning electron microscopy (SEM). Energy dispersive spectroscopy (EDS) maps of Zr or Al were collected for PVA/ZrO<sub>2</sub> and PVA/Al<sub>2</sub>O<sub>3</sub> mats, respectively. Melting temperature, melting enthalpy and crystallinity degree of the electrospun mats were determined by differential scanning calorimetry (DSC). Mechanical properties of electrospun mats were evaluated by uniaxial tensile test.

## 2. Experimental

## 2.1. Materials

Fully (99%) hydrolyzed PVA *M<sub>w</sub>* 130 000 (Aldrich), 5 wt% aqueous dispersion of ZrO<sub>2</sub> nanoparticles (average particle size 20 nm) (Aldrich), and 10 wt% aqueous dispersion of Al<sub>2</sub>O<sub>3</sub> nanoparticles (average particle size 20 nm) (Aldrich), were used as starting materials.

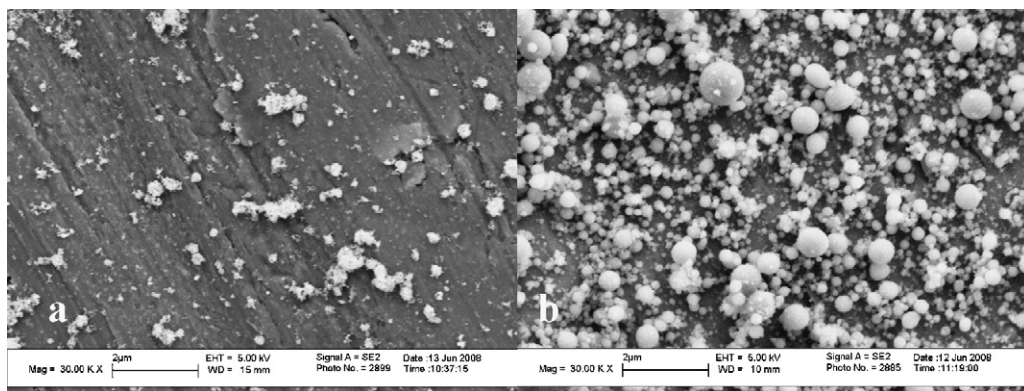
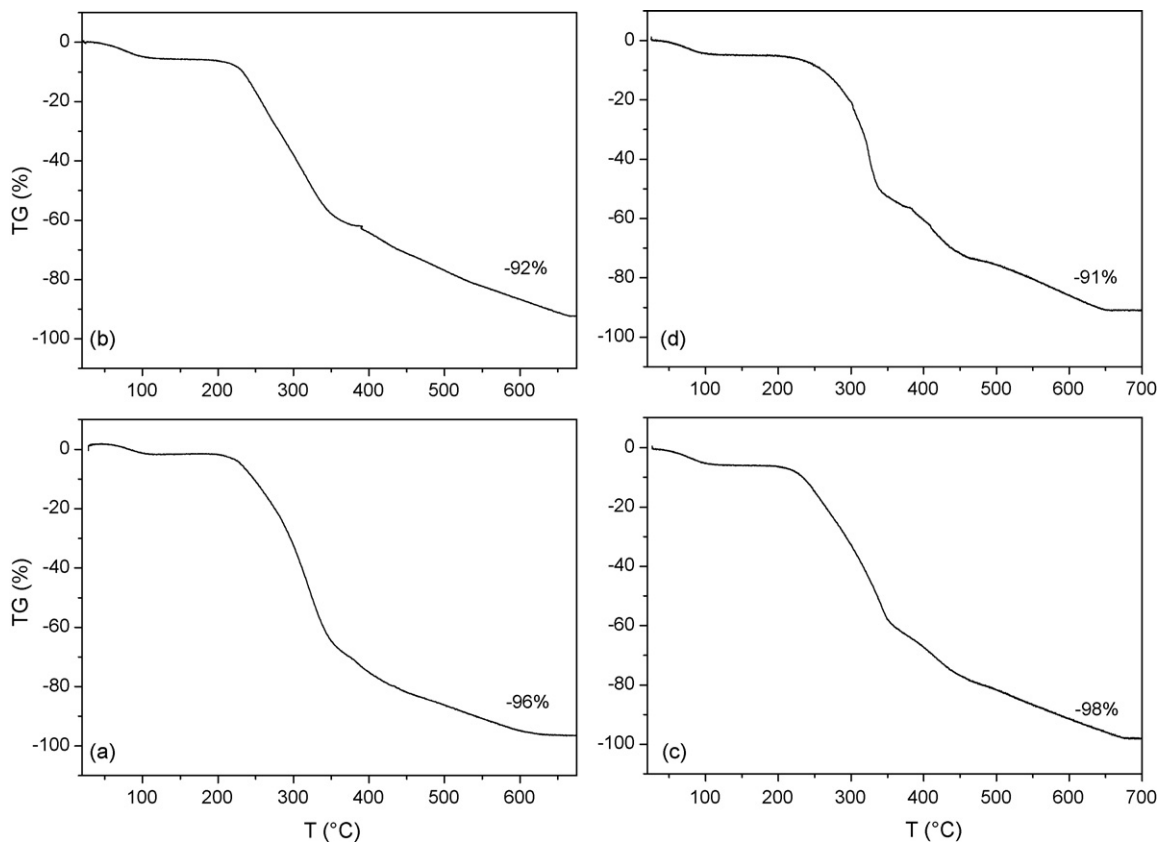
\* Corresponding author at: Dipartimento di Scienze e Tecnologie Chimiche, Università di Roma "Tor Vergata", Via della Ricerca Scientifica, 00133 Roma, Italy. Tel.: +39 06 72594273; fax: +39 06 72594328.

E-mail address: [Lamastra@scienze.uniroma2.it](mailto:Lamastra@scienze.uniroma2.it) (F.R. Lamastra).

**Table 1**

Viscosity, actual nanofiller content and thermal properties of neat and nanohybrid mats electrospun at 12 kV

Sample designation	Viscosity (mPa s)	Actual nanoparticle <sup>*</sup> content (wt%)	Thermal properties		
			$T_m$ (°C)	$\Delta H_m$ (J/g)	$X_c$ (%)
PVA	960	–	226 ± 1	74 ± 1	53
PVA/ZrO <sub>2</sub> -L	340	4 ± 1	227 ± 1	73 ± 1	55
PVA/ZrO <sub>2</sub> -H	1030	8 ± 1	229 ± 1	56 ± 1	44
PVA/Al <sub>2</sub> O <sub>3</sub> -L	890	2 ± 1	228 ± 1	75 ± 1	55
PVA/Al <sub>2</sub> O <sub>3</sub> -H	1300	9 ± 1	228 ± 1	55 ± 1	44

<sup>\*</sup> As-determined by TG analyses.**Fig. 1.** SEM micrographs of as-purchased aqueous dispersions of nanoparticles electrospun at 12 kV (a) ZrO<sub>2</sub> and (b) Al<sub>2</sub>O<sub>3</sub>.**Fig. 2.** TG curves of nanohybrid mats (a) PVA/ZrO<sub>2</sub>-L, (b) PVA/ZrO<sub>2</sub>-H, (c) PVA/Al<sub>2</sub>O<sub>3</sub>-L and (d) PVA/Al<sub>2</sub>O<sub>3</sub>-H.

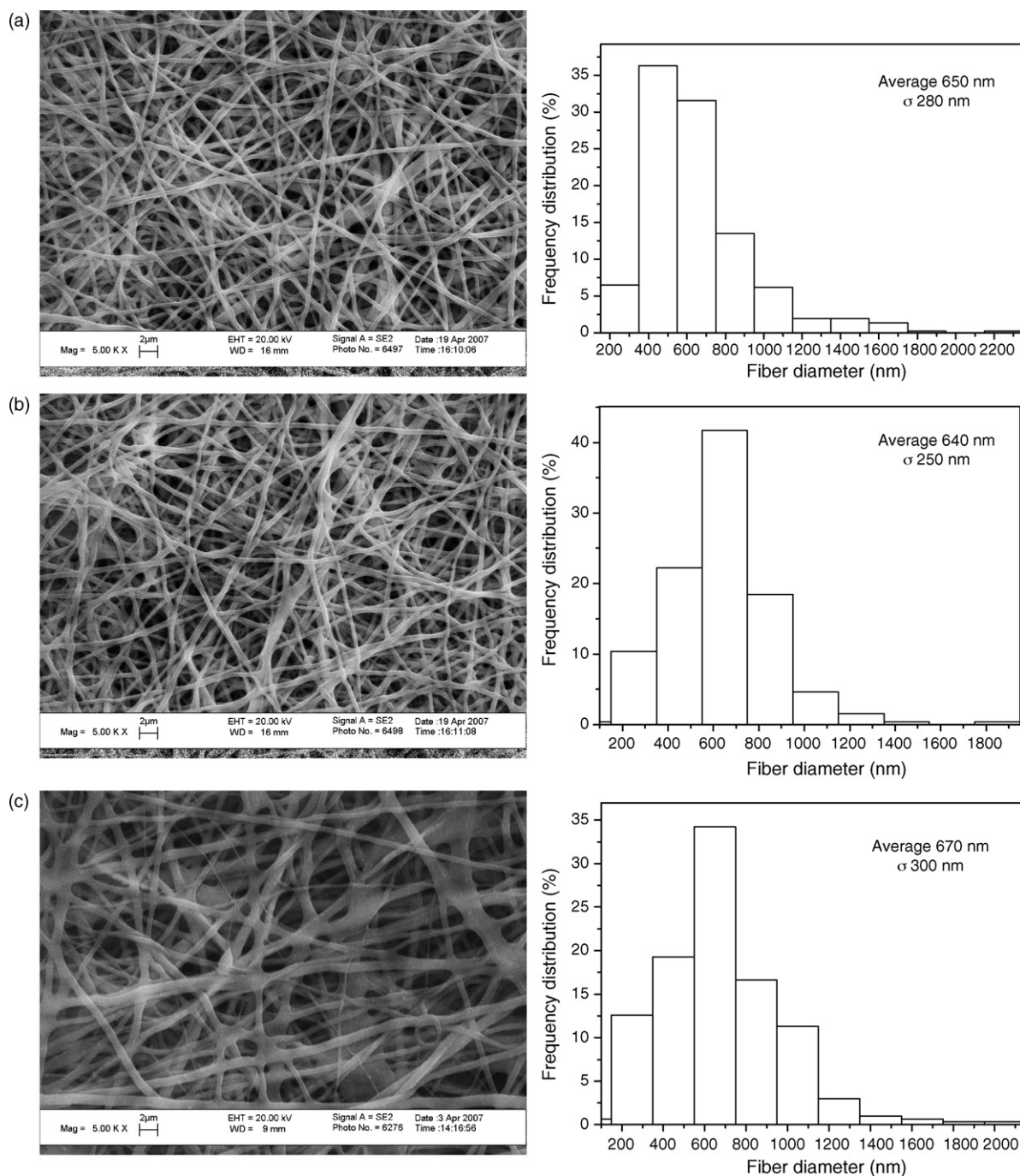


Fig. 3. SEM micrographs of neat PVA mat electrospun at (a) 12 kV, (b) 14 kV and (c) 16 kV.

## 2.2. Preparation of PVA/ZrO<sub>2</sub> and PVA/Al<sub>2</sub>O<sub>3</sub> suspensions

PVA solutions (8 wt%) were prepared dissolving PVA granules in deionized water at 80–90 °C for 2 h. Non-ionic surfactant Triton X-100 (1 wt%) (Aldrich) was added in order to lower the surface tension of the aqueous fully (99%) hydrolyzed PVA solution. The resulting mixture was then stirred 24 h at room temperature. Polymeric suspensions for electrospinning were obtained by adding the selected aqueous dispersion of nanoparticles to the PVA solution previously prepared. Two different nominal contents of ZrO<sub>2</sub> or Al<sub>2</sub>O<sub>3</sub> were considered, particularly 3 and 10% (w/w). Viscosity of the as-prepared solution and suspensions

was measured by a viscometer at 30 °C (Brookfield, Model DV-II).

## 2.3. Fabrication of nanohybrid fibrous mats by electrospinning

The suspension was poured in a syringe, the needle (18 gauge) being connected to the positive terminal of a high-voltage supply (Spellman SL30) able to generate DC voltages up to 30 kV. The suspension was delivered to the needle by a syringe pump (KD Scientific, USA). The distance between the tip of the needle and the aluminium collector (diameter 10 cm) was fixed at 10 cm. The following operative parameters were chosen: flow

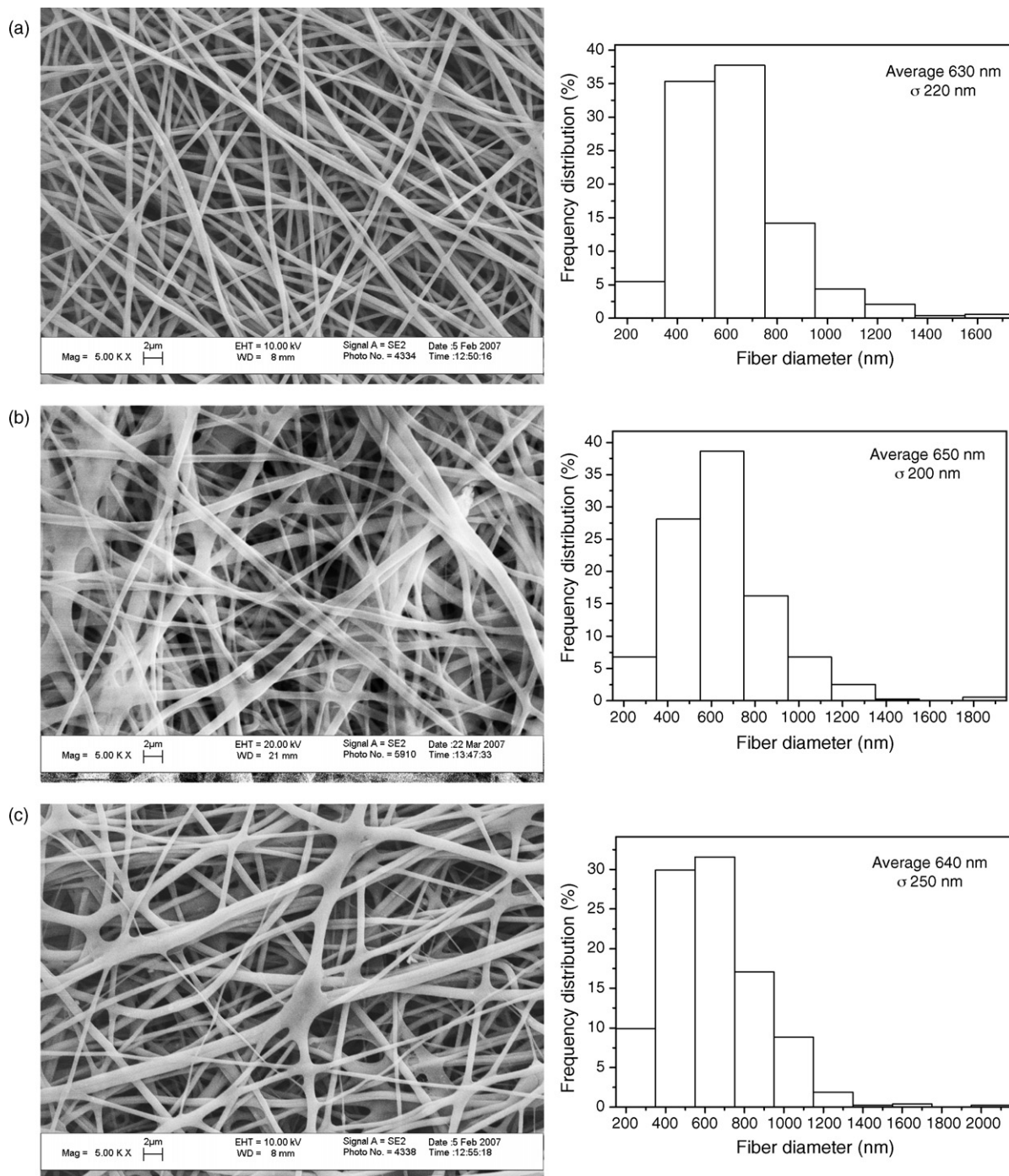


Fig. 4. SEM micrographs of PVA/ZrO<sub>2</sub>-L mat electrospun at (a) 12 kV, (b) 14 kV and (c) 16 kV.

rate 0.7 ml/h, applied voltage 12, 14 or 16 kV. Electrospun mats were soaked in methyl alcohol and dried for 48 h under vacuum.

#### 2.4. Electrospaying of as-purchased aqueous dispersions of nanoparticles

As-purchased aqueous dispersions (5 wt% ZrO<sub>2</sub> and 10 wt% Al<sub>2</sub>O<sub>3</sub>) were electrospayed at 12 kV, the other process parameters being the same used for the previously described electrospinning process.

#### 2.5. Characterisation techniques of electrospun mats

Aimed to evaluate the actual ceramic content of nanohybrid samples, thermogravimetry (TG) (*Netsch mod. STA 409*) was performed in the following conditions: air flow 80 cm<sup>3</sup>/min, peak temperature 700 °C, heating rate 5 °C/min, sample weight about 60 mg.

Fiber morphology, average fiber diameter and distribution were determined by scanning electron microscopy (*CAMBRIDGE STEREOSCAN 360 and Leo Supra 35*) on samples sputtered with gold.

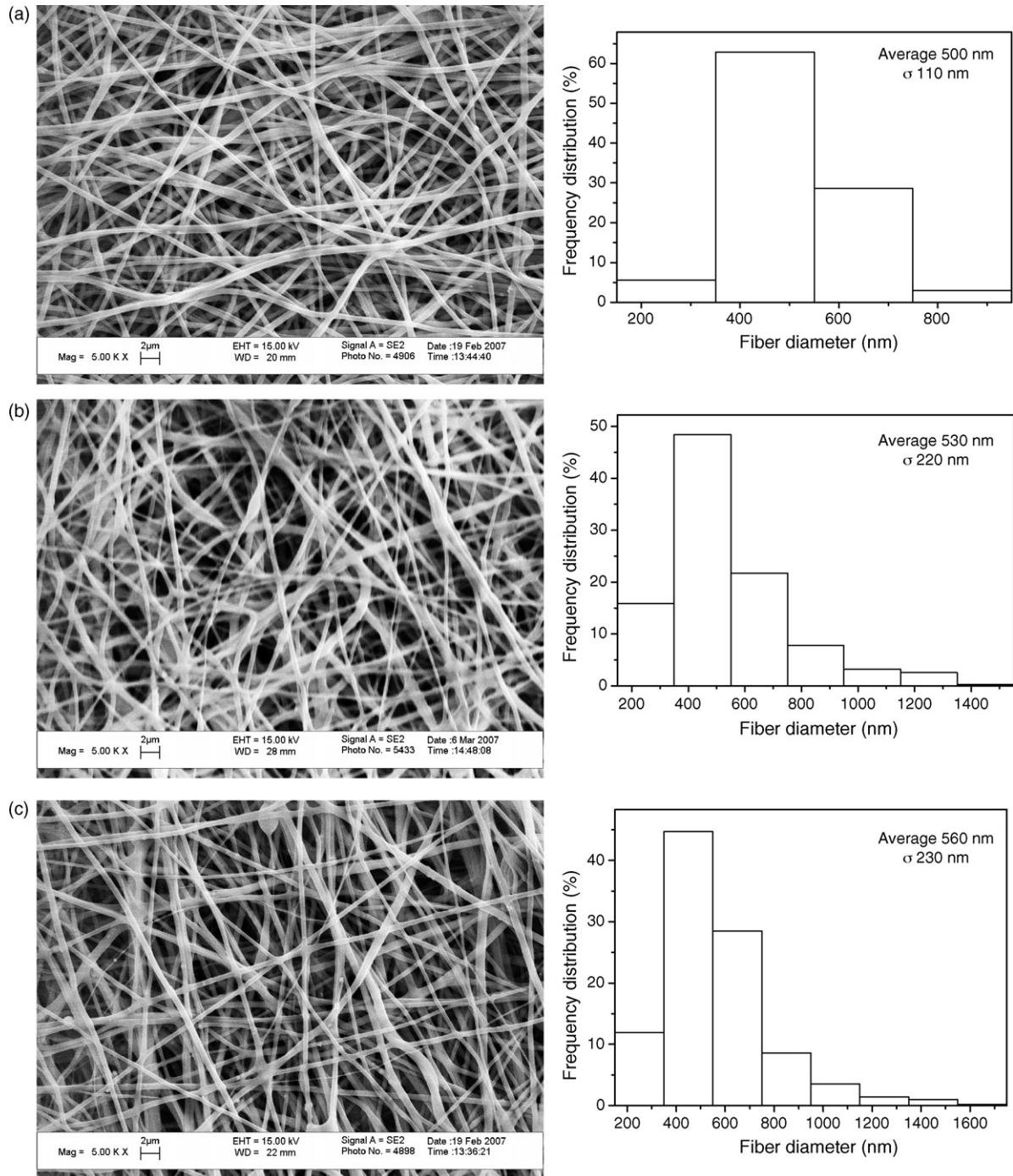


Fig. 5. SEM micrographs of PVA/Al<sub>2</sub>O<sub>3</sub>-L mat electrospun at (a) 12 kV, (b) 14 kV and (c) 16 kV.

In order to investigate the distribution of the ceramic phase within the polymeric mats, energy dispersive spectroscopy mapping of either Zr or Al (size 24.3 μm × 18.2 μm) was performed (INCA Energy 300, Oxford ELXII detector). EDS spectra were also performed on selected particles observed within the fibers. All EDS analyses were carried out on samples sputtered with graphite.

Melting temperature ( $T_m$ ) and melting enthalpy ( $\Delta H_m$ ) were determined by differential scanning calorimetry (Netzsch DSC200PC), considering the first heating scan (N<sub>2</sub> flow, temperature range 30–265 °C, heating rate 10 °C/min).

The crystallinity degree of electrospun samples was estimated as follows [9]:

$$X_c (\%) = \frac{\Delta H_m}{\Delta H_m^0(1-m)} \times 100, \quad (1)$$

where  $(1-m)$  is the actual weight fraction of PVA and  $\Delta H_m^0$  (J/g) = 138.6 for 100% crystalline PVA [6].

Mechanical properties were determined by uniaxial tensile test according to ASTM Standard D 1708. Measurements were carried out using an electromechanical testing machine (Texture Analyzer) equipped with 5 kg load cell. Samples were tested at break at

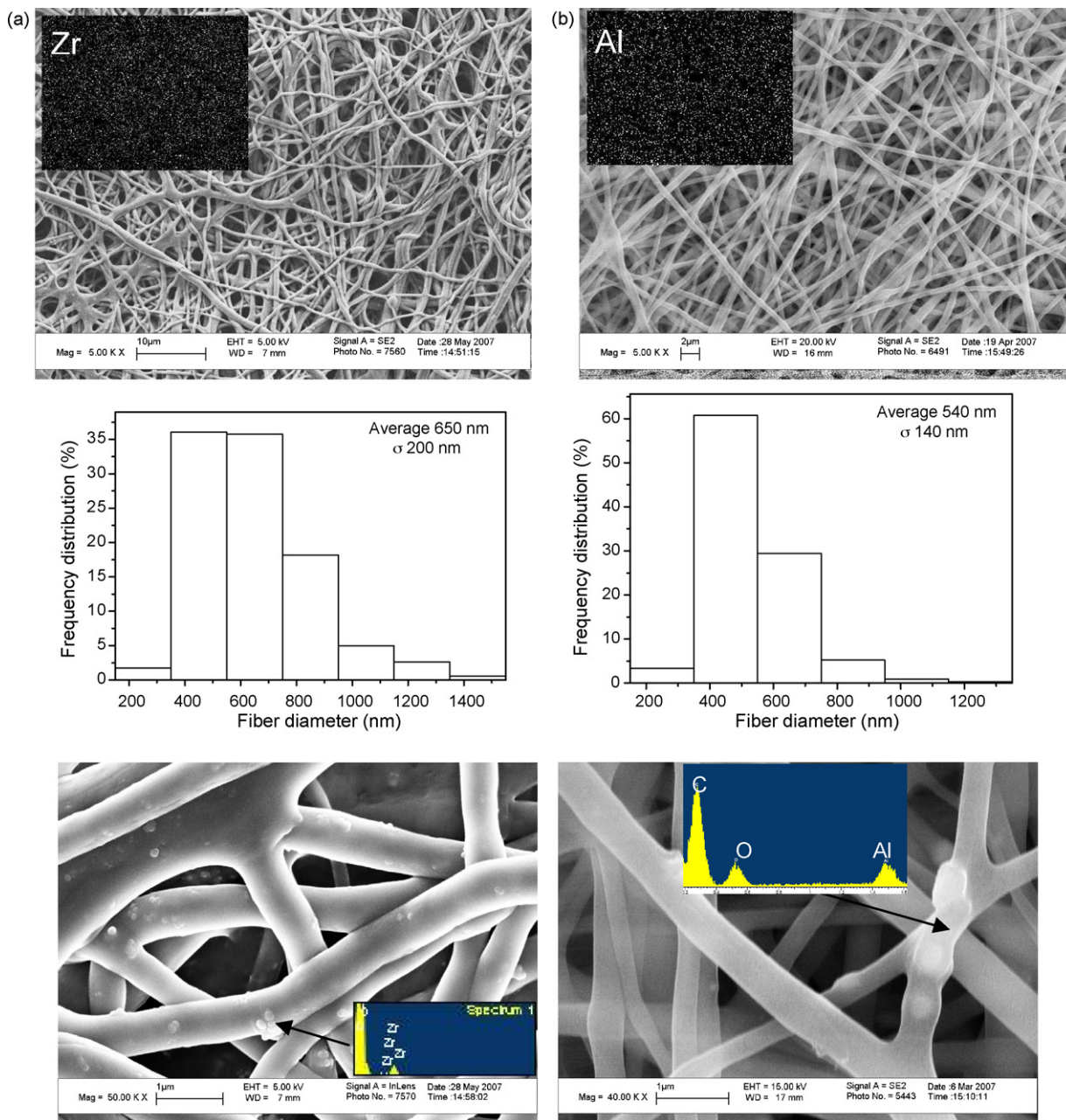


**Fig. 6.** SEM micrographs, EDS mapping (top insert frame) and EDS spectrum (bottom insert frame) of nanohybrid mats electrospun at 12 kV (a) PVA/ZrO<sub>2</sub>-H and (b) PVA/Al<sub>2</sub>O<sub>3</sub>-H.

1.2 mm/min. Tensile modulus, ultimate tensile stress, and strain to break were evaluated performing four tests for each sample.

### 3. Results and discussion

Results of viscosity measurements are reported in Table 1. The viscosity of suspensions containing low amounts of nanosized ZrO<sub>2</sub> or Al<sub>2</sub>O<sub>3</sub> (i.e. PVA/ZrO<sub>2</sub>-L and PVA/Al<sub>2</sub>O<sub>3</sub>-L) decreased with respect to the PVA solution. This result might be explained considering that nanoparticles place themselves among polymer chains, leading to reduced entanglements. According to the morphology of electro-sprayed aqueous dispersions (Fig. 1), this effect is more efficient in the case of the PVA/ZrO<sub>2</sub>-L suspension.

On the other side, in agreement with Wuttichareonmongkol et al. [10], PVA/ZrO<sub>2</sub>-H and PVA/Al<sub>2</sub>O<sub>3</sub>-H mixtures showed an

increased viscosity, this behaviour being again more remarkable for the polymeric suspension containing ZrO<sub>2</sub> nanoparticles (Table 1).

The TG curves of PVA/ZrO<sub>2</sub> and PVA/Al<sub>2</sub>O<sub>3</sub> electrospun mats are presented in Fig. 2, the resulting actual nanoparticle contents are reported in Table 1.

SEM micrographs of the neat electrospun PVA mat are reported in Fig. 3. The average fiber diameter was 650 ± 280, 640 ± 250 and 670 ± 300 nm for samples electrospun at 12, 14, and 16 kV, respectively. In Fig. 4, micrographs of nanohybrid PVA/ZrO<sub>2</sub>-L obtained at different voltage are presented. The average fiber diameter was 630 ± 220, 650 ± 200 and 640 ± 250 nm for samples electrospun at 12, 14, and 16 kV, respectively. In Fig. 5 SEM micrographs of PVA/Al<sub>2</sub>O<sub>3</sub>-L mats are reported. In this case, the average fiber size was 500 ± 110, 530 ± 220 and 560 ± 230 nm for samples electrospun at 12, 14, and 16 kV, respectively.

**Table 2**  
Mechanical properties of neat and nanohybrid mats electrospun at 12 kV

Sample designation	Tensile modulus (MPa)	Ultimate tensile stress (UTS) (MPa)	Strain to break ( $\epsilon_f$ ) (%)
PVA	90 ± 20	3.2 ± 0.2	90 ± 20
PVA/ZrO <sub>2</sub> -L	120 ± 45	5.4 ± 0.2	70 ± 5
PVA/ZrO <sub>2</sub> -H	190 ± 55	6.4 ± 0.6	70 ± 6
PVA/Al <sub>2</sub> O <sub>3</sub> -L	280 ± 80	5.4 ± 0.1	50 ± 10
PVA/Al <sub>2</sub> O <sub>3</sub> -H	350 ± 40	6 ± 2	60 ± 20

On the basis of these data, it resulted that the average fiber size of the PVA mat was comparable to that estimated for PVA/ZrO<sub>2</sub>-L and PVA/Al<sub>2</sub>O<sub>3</sub>-L nanohybrids. This result might be explained considering that all electrospun mats derived from solution or suspensions containing the same polymer to solvent ratio [11].

All these electrospun mats consisted of uniform, smooth fibers free of the defects forming a porous, highly interconnected architecture. Moreover, in the case of samples electrospun at 14 or 16 kV, some bundles and junctions were also evidenced. According to Ref. [12], this result might be associated to the decreased flight time of the electrospinning jet.

On this basis, nanohybrid samples containing high ceramic contents were produced at 12 kV (Table 1). In Fig. 6 the morphology of PVA/ZrO<sub>2</sub>-H and PVA/Al<sub>2</sub>O<sub>3</sub>-H are compared. The average fiber size (i.e. 650 ± 200 and 540 ± 140 nm, respectively), was not significantly different with respect to the other samples previously discussed.

EDS mappings showed that aluminium or zirconium were homogeneously distributed through the overall polymeric mat. Furthermore, nano and/or submicrometric agglomerates of ZrO<sub>2</sub> or Al<sub>2</sub>O<sub>3</sub> located onto and/or inside the polymeric fibers were evidenced (Fig. 6). Particularly, in the case of PVA/ZrO<sub>2</sub>-H sample, nanoparticles agglomerates ranging from 70 to 140 nm were observed. Bigger agglomerates of Al<sub>2</sub>O<sub>3</sub> (200–500 nm) were present in PVA/Al<sub>2</sub>O<sub>3</sub>-H mat.

In Table 1 are reported the melting temperature ( $T_m$ ), melting enthalpy ( $\Delta H_m$ ) and crystallinity degree ( $X_c$ ) of samples electrospun at 12 kV. In all cases,  $T_m$  ranged between 226 and 229 °C.

The melting enthalpy of PVA/ZrO<sub>2</sub>-L and PVA/Al<sub>2</sub>O<sub>3</sub>-L electrospun nanohybrids was comparable to that of the neat PVA mat. In the case of samples PVA/ZrO<sub>2</sub>-H and PVA/Al<sub>2</sub>O<sub>3</sub>-H, lower melting enthalpies were measured. This thermal behaviour has to be attributed to the interaction between the polymeric chains and the nanoparticles associated to the formation of hydrogen bonding between the polymer and the ceramic surface [13].

Furthermore, only PVA/ZrO<sub>2</sub>-H and PVA/Al<sub>2</sub>O<sub>3</sub>-H electrospun samples showed a significant difference in crystallinity degree (Table 1). Thus, the resulting  $X_c$  of the nanohybrid mats seems to be mainly driven by the amount of nanoparticles.

Mechanical properties of all electrospun nanohybrids and neat PVA are reported in Table 2.

As a general trend, the presence of ZrO<sub>2</sub> or Al<sub>2</sub>O<sub>3</sub> nanophase within the electrospun PVA fibers leads to a significant increase of tensile modulus and ultimate tensile stress accompanied by the decreasing of the strain to break. The effect is more evident in the case of PVA/Al<sub>2</sub>O<sub>3</sub> nanohybrids, suggesting a more efficient interdispersion of the ceramic nanophase associated to a stronger interphase.

#### 4. Conclusions

Nanohybrid fibrous PVA/ZrO<sub>2</sub> and PVA/Al<sub>2</sub>O<sub>3</sub> mats were obtained by electrospinning, the actual nanofiller content ranged between 2 and 9 wt%. The average fiber size was about 600 nm. The fiber diameter was not significantly affected by applied voltage (12, 14 and 16 kV) or nanofiller content. ZrO<sub>2</sub> and Al<sub>2</sub>O<sub>3</sub> nano and/or submicrometric agglomerates were located onto and/or inside the PVA fibers. The crystallinity degree of fibrous mats containing low amounts of ZrO<sub>2</sub> or Al<sub>2</sub>O<sub>3</sub> was around 55%, not significantly different with respect to the neat PVA sample. By increasing the ceramic nanoparticle content, the crystallinity degree decreased to about 44%. All electrospun nanohybrid mats showed improved mechanical properties, the effect being remarkable for the PVA/Al<sub>2</sub>O<sub>3</sub> system.

#### Acknowledgments

The Authors wish to thank Prof. V. Tagliaferri for differential scanning calorimetry measurements.

#### References

- [1] I. Chronakis, J. Mater. Process. Technol. 167 (2005) 283–293.
- [2] D. Li, Y. Xia, Adv. Mater. 16 (2004) 1151–1170.
- [3] A. Greiner, J.H. Wendorff, Angew. Chem. Int. Ed. 46 (2007) 5670–5703.
- [4] C. Shao, H.-Y. Kim, J. Gong, B. Ding, D.-R. Lee, S.-J. Park, Mater. Lett. 57 (2003) 1579–1584.
- [5] G. Mangiapia, R. Ricciardi, F. Auriemma, C. De Rosa, F. Lo Celso, R. Triolo, et al., J. Phys. Chem. B 111 (2007) 2166–2173.
- [6] L. Yao, T.W. Haas, A. Guiseppi-Elie, G.L. Bowlin, D.G. Simpson, G.E. Wnek, Chem. Mater. 15 (2003) 1860–1864.
- [7] M.G. Cascone, L. Lazzeri, E. Sparvoli, M. Scatena, L.P. Serino, S. Danti, J. Mater. Sci. Mater. Med. 5 (2004) 1309–1313.
- [8] M. Qi, Y. Gu, N. Sakata, D. Kim, Y. Shirouzu, C. Yamamoto, et al., Biomaterials 25 (2004) 5885–5892.
- [9] A. Arbeláiz, B. Fernández, A. Valea, I. Mondragon, Carbohydr. Polym. 64 (2006) 224–232.
- [10] P. Wutticharoenmongkol, N. Sanchavanakit, P. Pavasant, P. Supaphol, Macromol. Biosci. 6 (2006) 70–77.
- [11] A. Koski, K. Yim, S. Shivkumar, Mater. Lett. 58 (2004) 493–497.
- [12] S. Ramakrishna, K. Fujihara, W.E. Teo, T.C. Lim, Z. Ma, An introduction to Electrospinning and Nanofibers, World Scientific Publishing, Singapore, 2005, p. 104.
- [13] Z. Peng, D. Chen, J. Polym. Sci. B: Polym. Phys. 44 (2006) 534–540.